Cell Cycle 12:24, 3727–3735; December 15, 2013; © 2013 Landes Bioscience

On the origin of the stereoselective affinity of Nutlin-3 geometrical isomers for the MDM2 protein

Karim M ElSawy[1,2,*], Chandra S Verma[3,4,5,*], David P Lane[6], and Leo SD Caves[1,7,*]

[1]York Centre for Complex Systems Analysis (YCCSA); University of York; York, UK; [2]Department of Chemistry; College of Science; Qassim University; Saudi Arabia; [3]Bioinformatics Institute (A*STAR); Singapore; [4]Department of Biological Sciences; National University of Singapore; Singapore; [5]School of Biological Sciences; Nanyang Technological University; Singapore; [6]p53 Laboratory (A*STAR); Singapore; [7]Department of Biology; University of York; York, UK

The stereoselective affinity of small-molecule binding to proteins is typically broadly explained in terms of the thermodynamics of the final bound complex. Using Brownian dynamics simulations, we show that the preferential binding of the MDM2 protein to the geometrical isomers of Nutlin-3, an effective anticancer lead that works by inhibiting the interaction between the proteins p53 and MDM2, can be explained by kinetic arguments related to the formation of the MDM2:Nutlin-3 encounter complex. This is a diffusively bound state that forms prior to the final bound complex. We find that the MDM2 protein stereoselectivity for the Nutlin-3a enantiomer stems largely from the destabilization of the encounter complex of its mirror image enantiomer Nutlin-3b, by the K70 residue that is located away from the binding site. On the other hand, the trans-Nutlin-3a diastereoisomer exhibits a shorter residence time in the vicinity of MDM2 compared with Nutlin-3a due to destabilization of its encounter complex by the collective interaction of pairs of charged residues on either side of the binding site: Glu25 and Lys51 on one side, and Lys94 and Arg97 on the other side. This destabilization is largely due to the electrostatic potential of the trans-Nutlin-3a isomer being largely positive over extended continuous regions around its structure, which are otherwise well-identified into positive and negative regions in the case of the Nutlin-3a isomer. Such rich insight into the binding processes underlying biological selectivity complements the static view derived from the traditional thermodynamic analysis of the final bound complex. This approach, based on an explicit consideration of the dynamics of molecular association, suggests new avenues for kinetics-based anticancer drug development and discovery.

Keywords: Brownian dynamics simulation, MDM2 protein, nutlin stereoselectivity, stereoselectivity, encounter complex, kinetics-based drug discovery, residence time

*Correspondence to: Karim M ElSawy; Email: karim.elsawy@uniofyorkspace.net; Chandra S Verma: Email: chandra@bii.a-star.edu.sg; Leo SD Caves: Email: leo.caves@york.ac.uk

Submitted: 10/20/2013

Accepted: 11/19/2013

http://dx.doi.org/10.4161/cc.27273

Introduction

Symmetry is an important feature of biological systems, particularly at the molecular level.[1-4] A given topological configuration of a molecule can be identical in terms of composition, but can differ in its 3-dimensional structure in terms of spatial symmetry characteristics. In a chemical context, these structures are denoted as stereoisomers and may be broadly placed into 2 groups: enantiomers and diastereoisomers.[5-7] The stereochemistry of small molecules is key to their chemical reactivity and biological function.[8-10]

Interestingly, the stereochemical nature of drug molecules has been largely neglected in drug development strategies, with approximately 25% of marketed drugs[11] being generally racemates of synthetic chiral compounds, i.e., mixtures of stereoisomers rather than single chemical entities. Use of racemates as drugs can have several drawbacks in terms of adverse side effects and dosage.[12] However, the increasing availability of single-enantiomer drugs promises to provide clinicians with safer, better-tolerated, and more efficacious medications for treating patients.[13] For example, use of racemic dopa for the

treatment of Parkinson disease results in a number of adverse effects, including nausea, vomiting, anorexia, involuntary movements, and granulocytopenia.[14] In contrast, use of pure L-dopa isomer results in a reduction both in the dose required and in the number of patients experiencing adverse side effects.[15]

Recently, Nutlins (cis-4,5-Diaryl-2-imidazolines; **Fig. 1A and B**) have been shown to have potential to be developed as potent anticancer drug candidates.[16-20] Nutlins disrupt the binding of the E3-ligase MDM2 protein to the pro-apoptotic transcription factor p53, resulting in the activation of apoptotic pathways in cancer cells.[21] The corresponding trans-Nutlins (trans-4,5-Diaryl-2-imidazolines; **Fig. 1C and D**), however, have been found to inhibit the anti-apoptotic transcription factor NFkB concurrent with induction of programmed cell death, thus inhibiting anti-apoptotic pathways.[22] The enhanced efficacy of the cis-diastereisomer as an anticancer drug, compared with its trans isomer, has been confirmed by NMR-based screening.[23,24] Due to the asymmetry at the 4,5 diaryl substituent positions, each of the cis and trans isomers exists as a racemic mixture.

The different variants of Nutlin (Nutlin-1, Nutlin-2, and Nutlin-3)[19] assume similar binding modes when complexed to the MDM2 protein as revealed by X-ray crystallography[19,25] and NMR.[26] Nutlin-3 is the most biologically active among the Nutlin variants and is currently undergoing phase-I clinical trials as an anticancer lead candidate.[20] Nutlin-3a is a Nutlin-3 enantiomer, (–)-Nutlin-3, that is 150-fold more potent as an inhibitor of p53-MDM2 interactions than the other enantiomer, (+)-Nutlin-3, widely known as Nutlin-3b.[27] The designation of the Nutlin-3 enantiomers as Nutlin-3a and Nutlin-3b is based on the order of their peaks in chiral purification of racemic Nutlin, and the absolute configuration of the active Nutlin-3a enantiomer is largely not known.[28] Due to the lack of a crystal structure of Nultin-3 in complex with MDM2, the configuration of the Nutlin-2 enantiomer (Nutlin-3 analog with the 4-[S],5-[R]-imidazoline stereochemistry) bound to the MDM2 protein,[19] is commonly adopted as the active enantiomer in computational studies.[29-31]

The ability of proteins to discriminate between optical isomers is vital for living systems and is therefore exploited in drug design.[32,33] The stereospecificity of drug optical isomers viz. enantiomers, is usually explained on the basis of a 3-point attachment model[34] assuming a flat binding surface, or a 4-location model[35] for a more general binding mode. Both of these models employ thermodynamic arguments in order to explain the favorable binding of one optical isomer relative to the other.

Thermodynamic arguments have been widely used to rationalize the relative binding characteristics of molecular structures.[36] Indeed, the thermodynamic binding affinity is well established as the key biophysical parameter driving drug development. This thermodynamic approach implicitly assumes closed-system conditions, in which the target is exposed to an invariant concentration of the drug, and equilibrium is assumed.[37-40] However, in vivo conditions are very different, as the drug concentration is no longer invariant due to factors such as circulation, absorption, metabolism, and interaction with other cellular constituents.[39] Under these conditions, it is becoming increasingly clear that the kinetics of drug binding, as measured by the association and dissociation rate constants (k_{on} and k_{off}) of drug-target interactions are of significant relevance to biological activity.[39,41] For example, the development of resistance in EGFR has been associated with altered kinetics,[42] while p53 DNA site-specific recognition was found to rely more on differences in the kinetic off-rate rather than on differences in thermodynamic affinities of binding.[43] These observations, among others, have led a number of recent studies to stress a greater role for drug binding kinetics in therapeutic differentiation strategies,[44] thereby mitigating off-target mediated toxicity and leading to improved drug safety and tolerability.[41] It is becoming clear that the

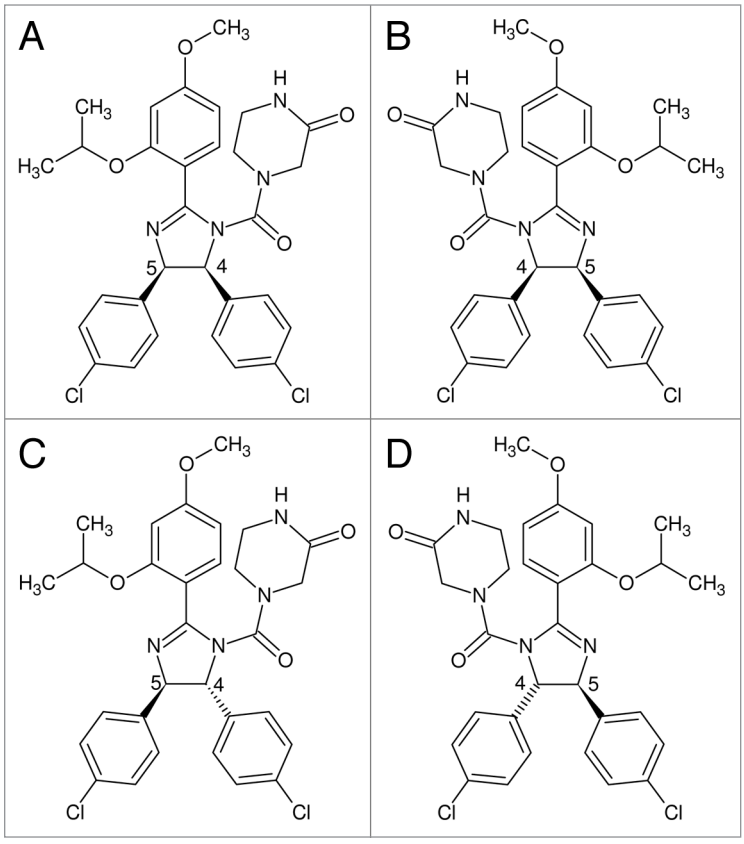

Figure 1. Four Nutlin-3 geometrical isomers: (**A**) Nutlin-3a, (**B**) Nutlin-3b, (**C**) trans-Nutlin-3a, and (**D**) trans-Nutlin-3b. The 4 geometrical isomers arise from asymmetry at the C4 and C5 positions of the imidazoline ring, resulting in the enantiomeric pairs of isomers a and b, and isomers c and d

off-rate k_{off} (or the drug-target residence time $\tau \sim 1/k_{off}$) is an important and perhaps crucial property for drug lead optimization,[37-39,41,45] thereby providing an alternative route to improving the therapeutic utility of a drug.[44]

In a previous work, we showed that the residence time of the drug protein encounter complex could be a crucial metric for explaining the preferential binding of Nutlin and p53 to the MDM2 protein.[46] In this work we focus on the origin of the difference in biological activity of the Nutlin-3 isomers. We employ the methodology we developed previously[46] to show that the preferential activity of the Nutlin-3 geometrical isomers toward the MDM2 protein can be explained, for the first time, in terms of differential binding kinetics. We perform Brownian dynamics (BD) simulations of the Nutlin-3 isomers and identify their encounter complexes with the MDM2 protein. We then compare the spatial densities of the diffusively bound ligands and their associated residence times to the known activity of the isomers. As a test of our hypotheses of the origin of differential binding, we perform mutations on the MDM2 protein in order to uncover the residues that are detrimental for the stereoselectivity of the MDM2 protein toward the Nutlin-3 isomers.

Results and Discussion

The diffusion characteristics of the Nulin-3 isomers toward the MDM2 protein were probed using a large number of BD trajectories (50 000 trajectories). Because of the asymmetry at the C4 and C5 positions on the Nutlin imidazoline ring, it was necessary to carry out the BD simulations for 4 different Nutlin-3 isomers (**Fig. 1**). Two of these isomers are enantiomers with a cis configuration at C4 and C5, which are widely known as Nutlin-3a and Nutlin-3b (**Fig. 1A and B**), while the other 2 are enantiomers of the trans isomer, which we will refer to

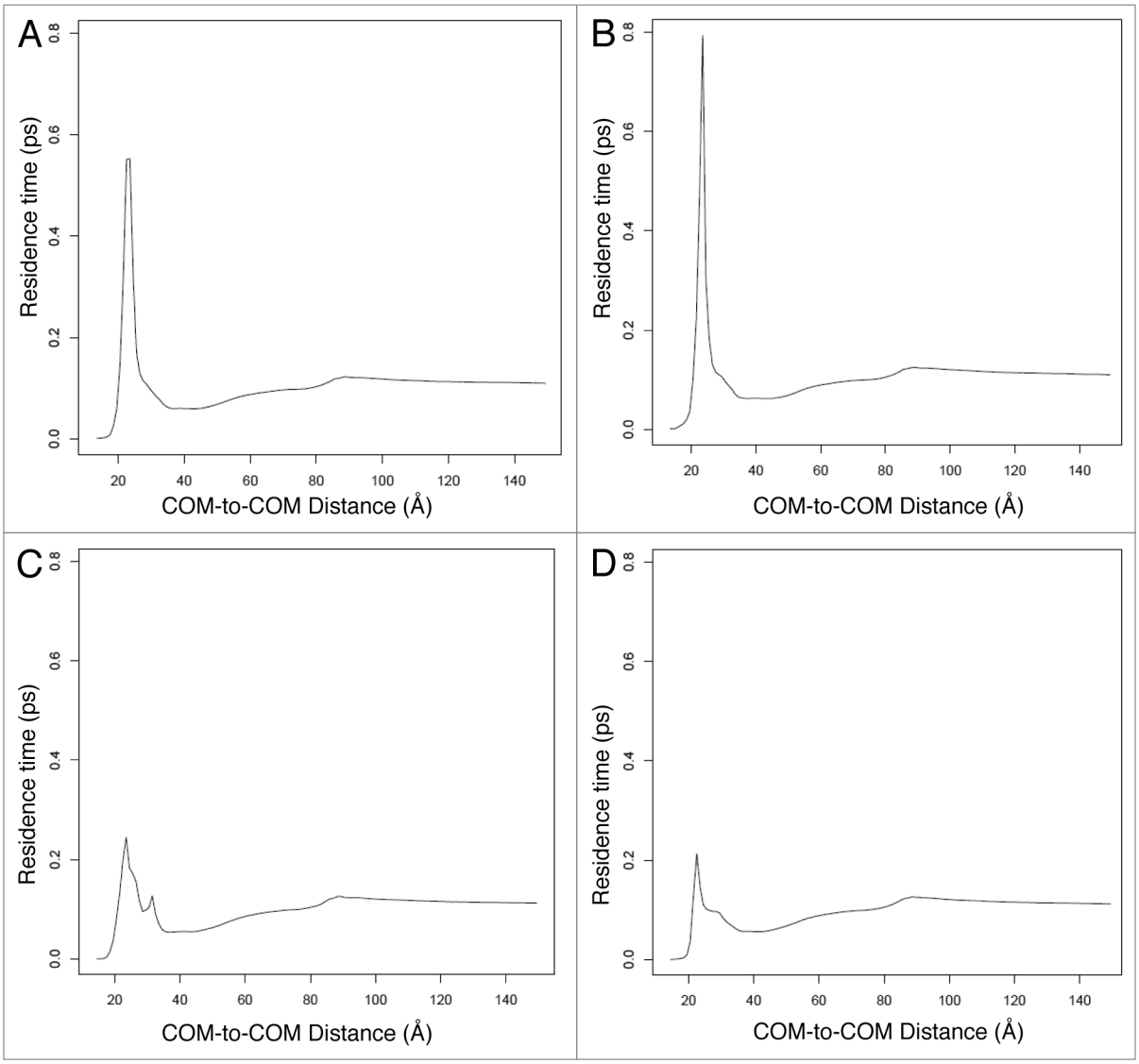

Figure 2. Radial profiles of the residence time of (**A**) Nutlin-3a, (**B**) Nutlin-3b, (**C**) trans-Nutlin-3a, and (**D**) trans-Nutlin-3b isomers relative to the distance between the center of mass (COM) of the isomer and the center of mass of the MDM2 protein. The residence time profiles were spatially normalized by dividing the total residence time at a radius r by the spherical volume slab $4\pi r^2$ and then averaged over the total number of Brownian dynamics trajectories, *N*.

throughout as trans-Nutlin-3a and trans-Nutlin-3b (**Fig. 1C and D**).

Radial residence time profiles of the Nutlin isomers around the MDM2 protein

Ligand residence time is increasingly being recognized as an important kinetic parameter that is directly related to biological activity in vivo.[37,39-41,45] Analysis of the diffusion trajectories of each of the Nutlin isomers toward the MDM2 protein reveals that the radial residence time profiles (**Fig. 2**) of the 2 trans-Nutlin-3 isomers are much lower than those of the cis isomers. The greater association of the cis isomers with MDM2 is consistent with the observed higher activity of the cis isomers relative to their trans counterparts.[23,24] The radial residence time profiles of the cis-isomers, however, shows that both Nutlin-3a and Nutlin-3b have very similar residence times around the MDM2 protein (verified by numerical integration of the radial residence time profiles).

Basins of attraction of Nutlin-3 isomers around the MDM2 protein

Identification of diffusive binding sites

Previously,[30,46] we showed how the ligand–protein encounter complex landscape can be partitioned into individual basins of attraction, defined as spatial regions that exhibit a higher rate of ligand association relative to the rate of ligand dissociation. Within the basins of attraction, the ligand experiences an enhanced residence time, such that they can be thought of as diffusive binding sites. The ligand receptor encounter complex is a precursor to any bound (non-diffusive) complex.[47,48] Unlike the bound complex, the encounter complex is stabilized mainly by long-range ligand-receptor electrostatic interactions[49] that dominate over other short-range interactions, such as van der Waals interactions and desolvation effects.

Nutlin-3a vs. Nutlin-3b

Comparison of the Nutiln-3a and Nutlin-3b behavior reveals that each of the isomers has 2 basins of attraction around the MDM2 protein with similar topography (**Fig. 3A and B**). However, there are differences: one of the basins of attraction of the Nutlin-3b isomer, the CTER basin, is more extended (relative to that of Nutlin-3a), with a taper toward the K70 residue and away from the Nutlin crystallographic binding site. This distinctive difference offers a potential explanation for the observed lower affinity of Nutlin-3b relative to Nutlin-3a[27] by providing a route for ligand depletion[50] away from the crystallographic binding site. Modeling the K70A mutation (**Fig. 3D**) results not only in the disappearance of the tapering end of the Nutlin-3b basin but, also, in the disappearance of the basin on the other side of the binding site, the NTER basin. This is suggestive of a flux between the 2 basins that is mediated by K70 and signals a crucial role for this residue in channeling Nutlin-3b around the MDM2 binding site. In contrast, for Nutlin-3a, the K70A mutation leads to complementary behavior, with the disappearance of the CTER basin of attraction with no effect on the NTER basin of attraction—on the other side of the binding site (**Fig. 3C**). The K70A results reveal that Nutlin-3a and its mirror image Nutlin-3b assume different modes of interaction with the MDM2 protein and suggest that Nutlin-3b has a higher mobility between the basins of attractions, while Nutlin-3a is more localized. Further testing of this hypothesis requires going beyond the time-averaged results we present here, to an extensive analysis of the dynamics of individual ligand trajectories (work in progress).

Nutlin-3a vs. trans-Nutlin-3a

Inspection of the basins of attraction of Nutlin-3a and trans-Nutlin-3a isomers (**Fig. 4A and C**) reveals that the Nutlin-3a isomer forms 2 basins of attraction, the CTER and NTER basins, in the vicinity of the MDM2 binding site. The trans-Nutlin-3a isomer, however, shows only 1 basin of attraction, the NTER basin, in a location similar to its Nutlin-3a

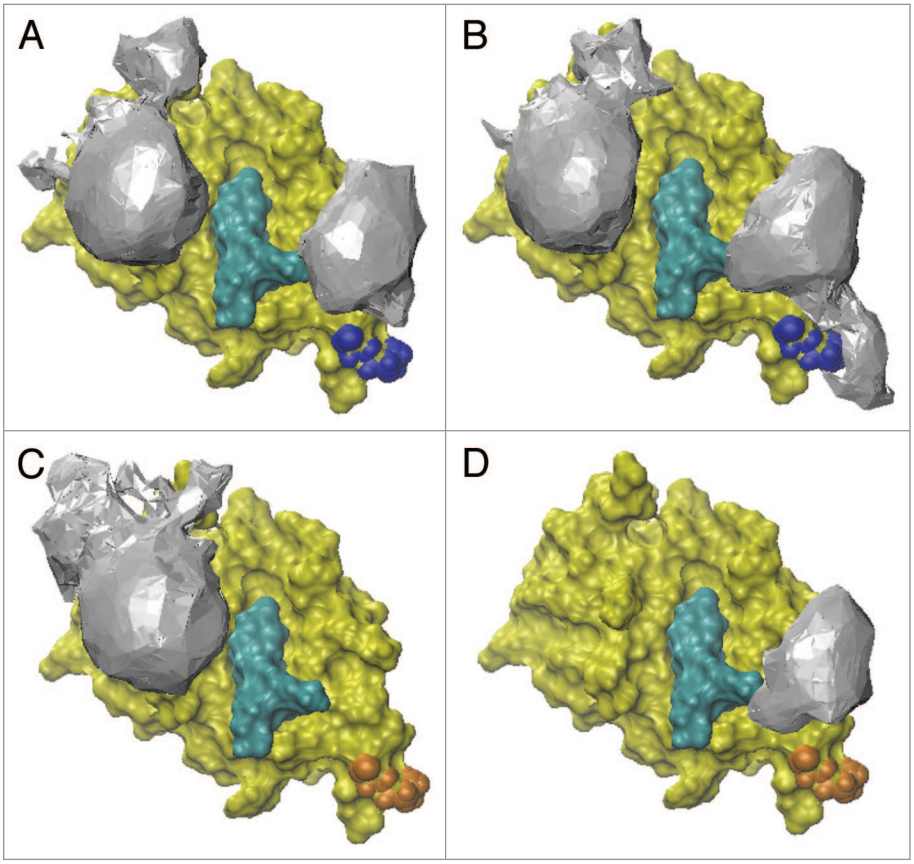

Figure 3. The basins of attraction of (**A**) Nutlin-3a and (**B**) Nutlin-3b enantiomers around the MDM2 protein (yellow) (PDBid 1YCR). The basins of attraction around the K70A MDM2 mutant of Nutlin-3a and Nutlin-3b are shown in (**C and D**). The MDM2 protein and its mutants are shown in yellow and the K70 residue is shown in blue. The K70A mutation is shown in brown in (**C and D**). For reference, Nutlin bound to the MDM2 binding site is shown in cyan. The basin of attraction that appears on the LHS of these figures is referred to as NTER in the text; the one on the RHS is referred to as CTER.

counterpart. Given the lack of any crystallographic structure of trans-Nutlin-3a bound to the MDM2 protein, this is suggestive that the NTER basin may not lead to the formation of a final bound complex. In order to investigate this further, we performed a series of simulations that involve mutations of the MDM2 charged residues that are located nearby the basins of attraction of Nutlin-3a.

Nutlin-3a and trans-Nutlin-3a basins of attraction around mutant MDM2 proteins

Previously[30] we showed that the Glu25 and Lys51 residues are important determinants of the topographical features of the electrostatic potential of the MDM2 protein that lead to channeling of Nutlin-2 (a close analog of Nutlin-3) directly toward the binding site through one of its basins of attraction (**Fig. 4A**; left column; NTER basin). Mutation of both Glu25 and Lys51 to alanine leads to a diminishing of the basins of attractions of both Nutlin-3a and trans-Nutlin-3a. It is interesting that although the Glu25 and Lys51 residues lie at one side of the binding site, their mutation leads to a diminishing of the 2 basins of attraction of Nutlin-3a, lying on 2 different sides of the binding site (**Fig. 4A**). The CTER basin of attraction, however, is in proximity to another pair of charged residues, Lys94 and Arg97 (**Fig. 4A**; left column; CTER basin), suggesting that interaction with these residues could be important for channeling Nutlin-3a and its trans isomer toward this basin. Mutation of Lys94 and Arg97 to alanine leads to the disappearance of both basins of attraction for Nutlin-3a and the appearance of only one basin of attraction, the NTER basin, for the trans-Nutlin-3a isomer (**Fig. 4A**). This indicates that Lys94 and Arg97 residues play a key role in stabilizing the channeling of Nutlin-3a toward the MDM2 binding site while destabilizing the channeling of the trans-Nutlin-3a isomer. The origin of this behavior can be traced to the topography of the electrostatic potential of the 2 isomers. Inspection of the projection of the electrostatic potential of Nutlin-3a and its trans isomer (**Fig. 5**) reveals that the Nutlin-3a isomer exhibits a single broad and intense region of positive potential, while the trans-Nutlin-3a isomer exhibits 2 connected regions of positive potential. The presence of these 2 regions of positive potential accounts for the destabilization of the trans isomer encounter complex by the positively charged Lys94 and Arg97 residues.

Conclusion

Brownian dynamics simulations were used to probe the diffusional encounters of Nutlin-3 geometrical isomers with the MDM2 protein. Characterization was principally through decomposition of the encounter complex landscape into basins of attraction, representing diffusive binding sites.

Both Nutlin-3a and 3b exhibit 2 distinct basins of attraction (NTER, CTER) that are situated either side of the observed binding site. Nutlin-3b shows a long taper on one of its basins (CTER) that extends away from the binding site. This taper is a potential channel for ligand depletion and may account for the observed low affinity of the Nutlin-3b enantiomer relative

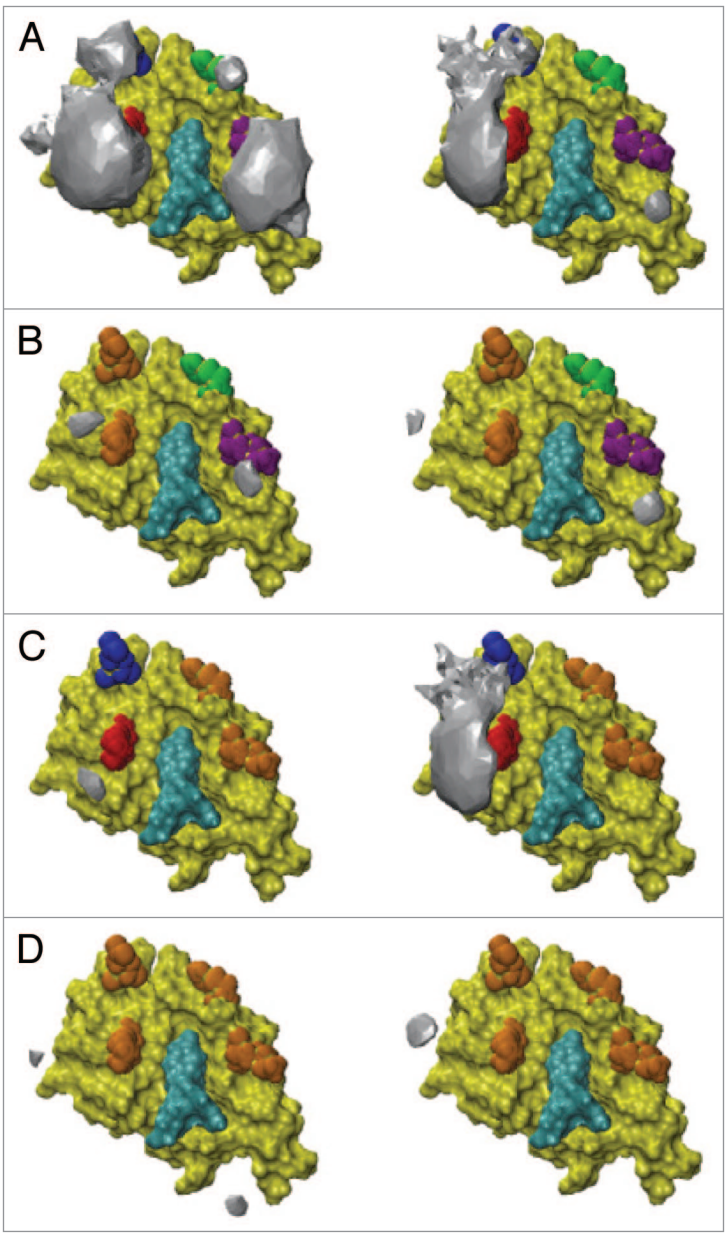

Figure 4. Basins of attraction (gray) of Nutlin-3a (left column) and trans-Nutlin-3a (right column) around: (**A**) wild-type MDM2, (**B**) MDM2 E25A/K51A, (**C**) MDM2 K94A/R97A, and (**D**) MDM2 E25A/K51A and K94A/R97A. The MDM2 protein and its mutants are shown in yellow. In wild-type MDM2 (panel a) the E25, K51, K94 and R97 residues are shown in blue, red, green, and violet, respectively. Upon mutation to alanine (**B–D**) these residues are shown in brown. For reference, Nutlin bound to the MDM2 binding site is shown in cyan (PDBid 1YCR).

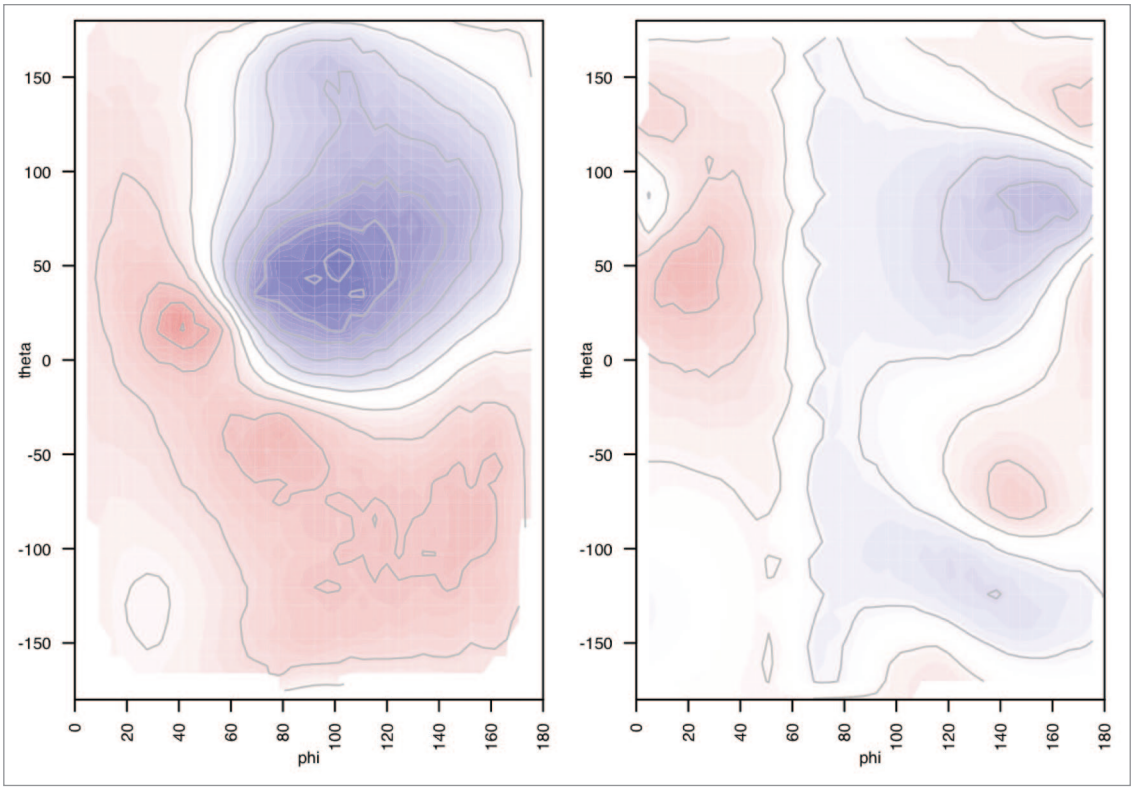

Figure 5. The average electrostatic potential of Nulin-3a (left) and trans-Nutlin-3a (right) in a 1-Å radial slab projected onto a plane defined by the phi and theta spherical coordinates of a 12-Å sphere, which is centered at the center of mass of each structure. The electrostatic potential color ramp changes smoothly from $-kT$ (red) to $+kT$ (blue) (kT is ~0.6 kcal mol^{-1} at 298K). The phi and theta angles are computed relative to orthogonal axes whose orientation was optimized as to minimize the RMSD between the 2 electrostatic potentials in the phi–theta plane.

to Nutlin-3a. We found that the K70A mutation had a pronounced effect on this binding behavior, selectively removing a different basin of attraction for each ligand (CTER for Nutlin-3a and NTER for Nutlin 3b).

Analysis of the encounter complex for the trans-Nutlin-3a diasteroisomer reveals a diminished residence time relative to Nutlin-3a. This difference manifests in trans-Nutlin-3a exhibiting only 1 basin of attraction (NTER) in the vicinity of the binding site rather than the 2 exhibited by Nutlin-3a.

Double alanine mutations of pairs of charged residues on either side of the binding site reveal that MDM2 interaction with the trans-Nutlin-3a isomer (presence of NTER basin of attraction) is stabilized by the electrostatic influence of Glu25 and Lys51. For the Nutlin-3a isomer, mutation of either pair of charged residues destabilizes its interaction with MDM2.

The picture that emerges is of a distribution of MDM2 surface residues, away from the binding site, that collectively channel Nutlin-3a into diffusive binding sites in the vicinity of the MDM2 binding site while serving to destabilize diffusional encounters with other Nutlin geometrical isomers. This, in part, explains the low affinity of these isomers for the MDM2 protein compared with Nutlin-3a[22-24,27] and likely accounts for the lack of crystal structure data of their complexes with MDM2.

This work is intended to demonstrate the kind of insight into the binding process that comes from an analysis of the diffusive binding in the encounter complex landscape. At present the analysis is focused on the location of distinct basins of attraction and their electrostatic determinants. Further work is necessary to fully exploit this dynamical approach, in terms of examining and quantifying the inter-basin dynamics of individual ligand trajectories, which will provide much more detailed insight. However, we hope the current results highlight the importance of kinetic considerations in pursuing a more detailed understanding of drug receptor interactions that accounts for affinity characteristics, even in the absence of traditional (non-diffusive) binding sites. Such an approach could be an important avenue for a new breed of kinetics-based drug discovery and development strategies.

Materials and Methods

Modeling the ligand protein diffusional association

Brownian dynamics simulations cannot account for the flexibility of the whole molecular system, and therefore we used a set of representative static structures for the MDM2 protein and the Nutlin-3 isomers. Fifteen snapshots of the MDM2 protein were extracted from an MD simulation of the Nutlin–MDM2 complex[31] and were used as the starting structures for the MDM2 protein in Brownian dynamics (BD) simulations. Representative structures of the Nutlin-3 isomers were obtained by analysis of MD trajectories of the isomers using the Merck Molecular Force Field (MMFF) within CHARMM.[51]

Table 1. The association schemes of MDM2 interaction with Nutlin-3 geometrical isomers

Protein	Ligand		Complex	Scheme
MDM2 +	Nutlin-3a	→	MDM2:Nutlin-3a	(1)
	Nutlin-3b	→	MDM2:Nutlin-3b	
MDM2 +	trans-Nutlin-3a	→	MDM2:trans-Nutlin-3a	(2)
	trans-Nutlin-3b	→	MDM2:trans-Nutlin-3b	

Principal component analysis (PCA) was used for constructing a collective coordinate subspace[52] for each Nutlin-3 isomer based on MD data wherein the isomer density was analyzed and partitioned into different basins using the contour following algorithm.[53] Structures corresponding to maximum density within each conformational basin were used as starting structures for the Nutlin-3 isomers in BD simulations.

BD simulations of the diffusional association of the Nutlin-3 enantiomers, (Nutin-3a and Nutlin-3b) and their trans diastereoisomers with the MDM2 protein were performed for the association schemes (1) and (2) (**Table 1**) using the SDA package.[54,55]

BD simulation details

The details of the BD simulations along with the algorithm for the identification of the basins of attraction were described previously[46] and are only outlined briefly here. The BD trajectories were generated by solving the translational and the rotational diffusion equations, using the Ermak–McCammon algorithm[56] as implemented in the SDA package version 4.23b. The translational and rotational diffusion coefficients were calculated using the HYDROPRO software.[57] Initially, the center of mass (COM) of the protein was placed at the origin, and the ligand was placed at b = 150.0 Å COM–COM separation relative to the protein COM. At this separation there is no preferential orientation of the ligands, since the electrostatic potential of the protein is nearly isotropic at distances of about 80 Å from their respective centers. A time step of 0.1 ps was used when the COM–COM separation of the 2 proteins was less than 90 Å. At larger separations, the time step was increased linearly, with a slope of 0.5 ps $Å^{-1}$. A total of 50 000 trajectories were run for each simulation; the simulations were terminated if the ligand–protein COM–COM separation exceeded $c = 3b$ Å.

The forces between the ligand and the protein derive from steric, desolvation, and electrostatic interactions. Steric interactions were implicitly taken into account by preventing the ligand and the protein from overlapping during the simulations using an exclusion grid centered at each of them with a grid spacing of 1 Å. The electrostatic force on any atom of the ligand was calculated by multiplying its charge by the electrostatic potential generated by the protein at that atom. The electrostatic potential around each protein was calculated by numerically solving the nonlinear Poisson–Boltzmann equation[58,59] on a 1 Å resolution grid with dimensions 161 × 161 × 161 Å centered on the ligand/protein using the APBS program.[60] The solvent dielectric constant was set to 78.5, the protein interior dielectric constant was set to 4, and the salt concentration was set to 0.15 M. Atomic charges and radii of the ligand and the protein were set using the PDB2PQR program.[61,62] The solute–solvent boundary was defined at the van der Waals surface, as the molecular surface definition was found to result in significant underestimation of the association rates in some cases.[63] Electrostatic desolvation was accounted for empirically by calculation of a desolvation penalty grid[64] around the ligand and the protein, using the SDA package. Consistent with the use of a van der Waals surface definition for the solute–solvent boundary, a scaling factor of 1.67 was used in the calculation of the desolvation grid.[63] For the sake of computational efficiency, the full set of atomic charges of the ligand and the protein was replaced during the BD simulations by a smaller set of effective charges that accurately reproduce their calculated electrostatic potential.[65] The effective charges were derived by the ECM module in the SDA package, so as to reproduce the electrostatic potential at the accessible surface (defined by a probe of 4 Å) in a 3-Å thick layer extending outwards from each structure.

The same BD simulation setup was used for simulations of MDM2 alanine mutants. The alanine mutations were performed by construction and optimization of sidechain orientation using the PDB2PQR program.[61,62]

Analysis of the BD simulations

From the BD trajectory data, the radial profiles of the ligand protein residence times were computed in spherical concentric radial slabs of 1 Å thickness that are centered at the center of mass of the protein. In order to get a detailed picture of the ligand protein interaction landscape, a 3D spatial probability density map was constructed around the protein by computing the average frequency of the ligand COM visiting individual grid cells using a grid of 1 Å resolution and dimensions 200 × 200 × 200 Å . The basins of attraction within the 3D grid were detected by the contour following algorithm described previously.[46,53]

Disclosure of Potential Conflicts of Interest

No potential conflicts of interest were disclosed.

Acknowledgment

We are very grateful to Drs Garib Murshudov and Seishi Shimizu for provision of computing resources.

References

1. Goodsell DS, Olson AJ. Structural symmetry and protein function. Annu Rev Biophys Biomol Struct 2000; 29:105-53; PMID:10940245; http://dx.doi.org/10.1146/annurev.biophys.29.1.105
2. Avetisov V, Goldanskii V. Mirror symmetry breaking at the molecular level. Proc Natl Acad Sci U S A 1996; 93:11435-42; PMID:8876153; http://dx.doi.org/10.1073/pnas.93.21.11435
3. Goodman G, Gershwin ME. The origin of life and the left-handed amino-acid excess: the furthest heavens and the deepest seas? Exp Biol Med (Maywood) 2006; 231:1587-92; PMID:17060678
4. Jorissen A, Cerf C. Asymmetric photoreactions as the origin of biomolecular homochirality: a critical review. Orig Life Evol Biosph 2002; 32:129-42; PMID:12185672; http://dx.doi.org/10.1023/A:1016087202273
5. Hill SA. Correct nomenclature for stereo isomers. Anaesthesia 2002; 57:200; PMID:11871988; http://dx.doi.org/10.1046/j.1365-2044.2002.2470_30.x
6. Cahn RS, Ingold C, Prelog V. Specification of Molecular Chirality. Angew Chem Int Ed Engl 1966; 5:385-415; http://dx.doi.org/10.1002/anie.196603851
7. Hirschmann H, Hanson KR. The differentiation of stereoheterotopic groups. Eur J Biochem 1971; 22:301-9; PMID:5125353; http://dx.doi.org/10.1111/j.1432-1033.1971.tb01545.x
8. Orr-Ewing AJ. Dynamical stereochemistry of bimolecular reactions. J Chem Soc, Faraday Trans 1996; 92:881-900; http://dx.doi.org/10.1039/ft9969200881
9. Kim YK, Arai MA, Arai T, Lamenzo JO, Dean EF 3rd, Patterson N, Clemons PA, Schreiber SL. Relationship of stereochemical and skeletal diversity of small molecules to cellular measurement space. J Am Chem Soc 2004; 126:14740-5; PMID:15535697; http://dx.doi.org/10.1021/ja048170p
10. Islam MR, Mahdi JG, Bowen ID. Pharmacological importance of stereochemical resolution of enantiomeric drugs. Drug Saf 1997; 17:149-65; PMID:9306051; http://dx.doi.org/10.2165/00002018-199717030-00002
11. Hutt AJ. The development of single-isomer molecules: why and how. CNS Spectr 2002; 7(Suppl 1):14-22; PMID:15131488
12. Nguyen LA, He H, Pham-Huy C. Chiral drugs: an overview. Int J Biomed Sci 2006; 2:85-100; PMID:23674971
13. McConathy J, Owens MJ. Stereochemistry in Drug Action. Prim Care Companion J Clin Psychiatry 2003; 5:70-3; PMID:15156233; http://dx.doi.org/10.4088/PCC.v05n0202
14. Cotzias GC, Van Woert MH, Schiffer LM. Aromatic amino acids and modification of parkinsonism. N Engl J Med 1967; 276:374-9; PMID:5334614; http://dx.doi.org/10.1056/NEJM196702162760703
15. Cotzias GC, Papavasiliou PS, Gellene R. Modification of Parkinsonism--chronic treatment with L-dopa. N Engl J Med 1969; 280:337-45; PMID:4178641; http://dx.doi.org/10.1056/NEJM196902132800701
16. Brown CJ, Cheok CF, Verma CS, Lane DP. Reactivation of p53: from peptides to small molecules. Trends Pharmacol Sci 2011; 32:53-62; PMID:21145600; http://dx.doi.org/10.1016/j.tips.2010.11.004
17. Vassilev LT. MDM2 inhibitors for cancer therapy. Trends Mol Med 2007; 13:23-31; PMID:17126603; http://dx.doi.org/10.1016/j.molmed.2006.11.002
18. Verma R, Rigatti MJ, Belinsky GS, Godman CA, Giardina C. DNA damage response to the Mdm2 inhibitor nutlin-3. Biochem Pharmacol 2010; 79:565-74; PMID:19788889; http://dx.doi.org/10.1016/j.bcp.2009.09.020
19. Vassilev LT, Vu BT, Graves B, Carvajal D, Podlaski F, Filipovic Z, Kong N, Kammlott U, Lukacs C, Klein C, et al. In vivo activation of the p53 pathway by small-molecule antagonists of MDM2. Science 2004; 303:844-8; PMID:14704432; http://dx.doi.org/10.1126/science.1092472
20. Secchiero P, Bosco R, Celeghini C, Zauli G. Recent advances in the therapeutic perspectives of Nutlin-3. Curr Pharm Des 2011; 17:569-77; PMID:21391907; http://dx.doi.org/10.2174/138161211795222586
21. Kojima K, Konopleva M, Samudio IJ, Shikami M, Cabreira-Hansen M, McQueen T, Ruvolo V, Tsao T, Zeng Z, Vassilev LT, et al. MDM2 antagonists induce p53-dependent apoptosis in AML: implications for leukemia therapy. Blood 2005; 106:3150-9; PMID:16014563; http://dx.doi.org/10.1182/blood-2005-02-0553
22. Sharma V, Peddibhotla S, Tepe JJ. Sensitization of cancer cells to DNA damaging agents by imidazolines. J Am Chem Soc 2006; 128:9137-43; PMID:16834387; http://dx.doi.org/10.1021/ja060273f
23. Srivastava S, Beck B, Wang W, Czarna A, Holak TA, Dömling A. Rapid and efficient hydrophilicity tuning of p53/mdm2 antagonists. J Comb Chem 2009; 11:631-9; PMID:19548636; http://dx.doi.org/10.1021/cc9000218
24. Czarna A, Beck B, Srivastava S, Popowicz GM, Wolf S, Huang Y, Bista M, Holak TA, Dömling A. Robust generation of lead compounds for protein-protein interactions by computational and MCR chemistry: p53/Hdm2 antagonists. Angew Chem Int Ed Engl 2010; 49:5352-6; PMID:20575124; http://dx.doi.org/10.1002/anie.201001343
25. Anil B, Riedinger C, Endicott JA, Noble ME. The structure of an MDM2-Nutlin-3a complex solved by the use of a validated MDM2 surface-entropy reduction mutant. Acta Crystallogr D Biol Crystallogr 2013; 69:1358-66; PMID:23897459; http://dx.doi.org/10.1107/S0907444913004459
26. Fry DC, Emerson SD, Palme S, Vu BT, Liu CM, Podlaski F. NMR structure of a complex between MDM2 and a small molecule inhibitor. J Biomol NMR 2004; 30:163-73; PMID:15557803; http://dx.doi.org/10.1023/B:JNMR.0000048856.84603.9b
27. Fischer PM. Peptide, Peptidomimetic, and Small-molecule Antagonists of the p53-HDM2 Protein-Protein Interaction. Int J Pept Res Ther 2006; 12:3-19; PMID:19617922; http://dx.doi.org/10.1007/s10989-006-9016-5
28. Davis TA, Johnston JN. Catalytic, Enantioselective Synthesis of Stilbene cis-Diamines: A Concise Preparation of (-)-Nutlin-3, a Potent p53/MDM2 Inhibitor. Chem Sci 2011; 2:1076-9; PMID:22708054; http://dx.doi.org/10.1039/c1sc00061f
29. Joseph TL, Madhumalar A, Brown CJ, Lane DP, Verma CS. Differential binding of p53 and nutlin to MDM2 and MDMX: computational studies. Cell Cycle 2010; 9:1167-81; PMID:20190571; http://dx.doi.org/10.4161/cc.9.6.11067
30. ElSawy KM, Verma CS, Joseph TL, Lane DP, Twarock R, Caves LS. On the interaction mechanisms of a p53 peptide and nutlin with the MDM2 and MDMX proteins: a Brownian dynamics study. Cell Cycle 2013; 12:394-404; PMID:23324352; http://dx.doi.org/10.4161/cc.23511
31. Dastidar SG, Lane DP, Verma CS. Modulation of p53 binding to MDM2: computational studies reveal important roles of Tyr100. BMC Bioinformatics 2009; 10(Suppl 15):S6; PMID:19958516; http://dx.doi.org/10.1186/1471-2105-10-S15-S6
32. Burke D, Henderson DJ. Chirality: a blueprint for the future. Br J Anaesth 2002; 88:563-76; PMID:12066734; http://dx.doi.org/10.1093/bja/88.4.563
33. Brooks WH, Guida WC, Daniel KG. The significance of chirality in drug design and development. Curr Top Med Chem 2011; 11:760-70; PMID:21291399; http://dx.doi.org/10.2174/156802611795165098
34. Ogston AG. Interpretation of experiments on metabolic processes, using isotopic tracer elements. Nature 1948; 162:963; PMID:18225319; http://dx.doi.org/10.1038/162963b0
35. Mesecar AD, Koshland DE Jr. A new model for protein stereospecificity. Nature 2000; 403:614-5; PMID:10688187
36. Henrich S, Salo-Ahen OM, Huang B, Rippmann FF, Cruciani G, Wade RC. Computational approaches to identifying and characterizing protein binding sites for ligand design. J Mol Recognit 2010; 23:209-19; PMID:19746440
37. Lu H, Tonge PJ. Drug-target residence time: critical information for lead optimization. Curr Opin Chem Biol 2010; 14:467-74; PMID:20663707; http://dx.doi.org/10.1016/j.cbpa.2010.06.176
38. Swinney DC. The role of binding kinetics in therapeutically useful drug action. Curr Opin Drug Discov Devel 2009; 12:31-9; PMID:19152211
39. Copeland RA, Pompliano DL, Meek TD. Drug-target residence time and its implications for lead optimization. Nat Rev Drug Discov 2006; 5:730-9; PMID:16888652; http://dx.doi.org/10.1038/nrd2082
40. Tummino PJ, Copeland RA. Residence time of receptor-ligand complexes and its effect on biological function. Biochemistry 2008; 47:5481-92; PMID:18412369; http://dx.doi.org/10.1021/bi8002023
41. Copeland RA. The dynamics of drug-target interactions: drug-target residence time and its impact on efficacy and safety. Expert Opin Drug Discov 2010; 5:305-10; PMID:22823083; http://dx.doi.org/10.1517/17460441003677725
42. Yun C-H, Mengwasser KE, Toms AV, Woo MS, Greulich H, Wong K-K, Meyerson M, Eck MJ. The T790M mutation in EGFR kinase causes drug resistance by increasing the affinity for ATP. Proc Natl Acad Sci U S A 2008; 105:2070-5; PMID:18227510; http://dx.doi.org/10.1073/pnas.0709662105
43. Petty TJ, Emamzadah S, Costantino L, Petkova I, Stavridi ES, Saven JG, Vauthey E, Halazonetis TD. An induced fit mechanism regulates p53 DNA binding kinetics to confer sequence specificity. EMBO J 2011; 30:2167-76; PMID:21522129; http://dx.doi.org/10.1038/emboj.2011.127
44. Swinney DC. Applications of Binding Kinetics to Drug Discovery: Translation of Binding Mechanisms to Clinically Differentiated Therapeutic Responses. Pharmaceutical Medicine 2008; 22:23-34; http://dx.doi.org/10.1007/BF03256679
45. Zhang R, Monsma F. The importance of drug-target residence time. Curr Opin Drug Discov Devel 2009; 12:488-96; PMID:19562645
46. ElSawy KM, Twarock R, Lane DP, Verma CS, Caves LSD. Characterization of the Ligand Receptor Encounter Complex and Its Potential for in Silico Kinetics-Based Drug Development. J Chem Theory Comput 2012; 8:314-21; http://dx.doi.org/10.1021/ct200560w
47. Gabdoulline RR, Wade RC. On the protein-protein diffusional encounter complex. J Mol Recognit 1999; 12:226-34; PMID:10440993; http://dx.doi.org/10.1002/(SICI)1099-1352(199907/08)12:4<226::AID-JMR462>3.0.CO;2-P
48. Tang C, Iwahara J, Clore GM. Visualization of transient encounter complexes in protein-protein association. Nature 2006; 444:383-6; PMID:17051159; http://dx.doi.org/10.1038/nature05201

49. Suh JY, Tang C, Clore GM. Role of electrostatic interactions in transient encounter complexes in protein-protein association investigated by paramagnetic relaxation enhancement. J Am Chem Soc 2007; 129:12954-5; PMID:17918946; http://dx.doi.org/10.1021/ja0760978
50. Edelstein SJ, Stefan MI, Le Novère N. Ligand depletion in vivo modulates the dynamic range and cooperativity of signal transduction. PLoS One 2010; 5:e8449; PMID:20052284; http://dx.doi.org/10.1371/journal.pone.0008449
51. Brooks BR, Brooks CL 3rd, Mackerell AD Jr., Nilsson L, Petrella RJ, Roux B, Won Y, Archontis G, Bartels C, Boresch S, et al. CHARMM: the biomolecular simulation program. J Comput Chem 2009; 30:1545-614; PMID:19444816; http://dx.doi.org/10.1002/jcc.21287
52. Caves LSD, Evanseck JD, Karplus M. Locally accessible conformations of proteins: multiple molecular dynamics simulations of crambin. Protein Sci 1998; 7:649-66; PMID:9541397; http://dx.doi.org/10.1002/pro.5560070314
53. Elsawy KM, Hodgson MK, Caves LSD. The physical determinants of the DNA conformational landscape: an analysis of the potential energy surface of single-strand dinucleotides in the conformational space of duplex DNA. Nucleic Acids Res 2005; 33:5749-62; PMID:16214808; http://dx.doi.org/10.1093/nar/gki888
54. Gabdoulline RR, Wade RC. Simulation of the diffusional association of barnase and barstar. Biophys J 1997; 72:1917-29; PMID:9129797; http://dx.doi.org/10.1016/S0006-3495(97)78838-6
55. Gabdoulline RR, Wade RC. Brownian dynamics simulation of protein-protein diffusional encounter. Methods 1998; 14:329-41; PMID:9571088; http://dx.doi.org/10.1006/meth.1998.0588
56. Donald LE, McCammon JA. Brownian dynamics with hydrodynamic interactions. J Chem Phys 1978; 69:1352-60; http://dx.doi.org/10.1063/1.436761
57. García De La Torre J, Huertas ML, Carrasco B. Calculation of hydrodynamic properties of globular proteins from their atomic-level structure. Biophys J 2000; 78:719-30; PMID:10653785; http://dx.doi.org/10.1016/S0006-3495(00)76630-6
58. Im W, Beglov D, Roux B. Continuum Solvation Model: computation of electrostatic forces from numerical solutions to the Poisson-Boltzmann equation. Comput Phys Commun 1998; 111:59-75; http://dx.doi.org/10.1016/S0010-4655(98)00016-2
59. Coalson R, Beck TL. Numerical Methods for Solving Poisson and Poisson-Boltzmann Type Equations. In: von Rague Schleyer P, ed. Encyclopedia of Computational Chemistry. New York: John-Wiley, 1998:2086-100.
60. Baker NA, Sept D, Joseph S, Holst MJ, McCammon JA. Electrostatics of nanosystems: application to microtubules and the ribosome. Proc Natl Acad Sci U S A 2001; 98:10037-41; PMID:11517324; http://dx.doi.org/10.1073/pnas.181342398
61. Dolinsky TJ, Czodrowski P, Li H, Nielsen JE, Jensen JH, Klebe G, Baker NA. PDB2PQR: expanding and upgrading automated preparation of biomolecular structures for molecular simulations. Nucleic Acids Res 2007; 35:W522-5; PMID:17488841; http://dx.doi.org/10.1093/nar/gkm276
62. Czodrowski P, Dramburg I, Sotriffer CA, Klebe G. Development, validation, and application of adapted PEOE charges to estimate pKa values of functional groups in protein–ligand complexes. Proteins: Struct, Funct. Bioinf 2006; 65:424-37
63. Gabdoulline RR, Wade RC. Protein-protein association: investigation of factors influencing association rates by brownian dynamics simulations. J Mol Biol 2001; 306:1139-55; PMID:11237623; http://dx.doi.org/10.1006/jmbi.2000.4404
64. Elcock AH, Gabdoulline RR, Wade RC, McCammon JA. Computer simulation of protein-protein association kinetics: acetylcholinesterase-fasciculin. J Mol Biol 1999; 291:149-62; PMID:10438612; http://dx.doi.org/10.1006/jmbi.1999.2919
65. Gabdoulline RR, Wade RC. Effective Charges for Macromolecules in Solvent. J Phys Chem 1996; 100:3868-78; http://dx.doi.org/10.1021/jp953109f